RESEARCH ARTICLE



WILEY

Transpiration and subsurface controls of streamflow recession characteristics

Arik Tashie¹ | Charles I. Scaife² | Lawrence E. Band^{2,3}

Correspondence

Arik Tashie, Department of Geological Sciences, University of North Carolina at Chapel Hill, Chapel Hill, NC. Email: arik@live.unc.edu

Funding information

National Science Foundation Long-Term Ecological Research, Grant/Award Number: DEB-0823293

Abstract

In headwater catchments, streamflow recedes between periods of rainfall at a predictable rate generally defined by a power-law relationship relating streamflow decay to streamflow. Research over the last four decades has applied this relationship to predictions of water resource availability as well as estimations of basin-wide physiographic characteristics and ecohydrologic conditions. However, the interaction of biophysical processes giving rise to the form of these power-law relationships remains poorly understood, and recent investigations into the variability of streamflow recession characteristics between discrete events have alternatively suggested evapotranspiration, water table elevation, and stream network contraction as dominant factors, without consensus. To assess potential temporal variability and interactions in the mechanism(s) driving streamflow recession, we combine long-term observational data from a headwater stream in the southern Appalachian Mountains with state and flux conditions from a process-based ecohydrologic model. Streamflow recession characteristics are nonunique and vary systematically with seasonal fluctuations in both rates of transpiration and watershed wetness conditions, such that transpiration dominates recession signals in the early growing season and diminishes in effect as the water table elevation progressively drops below and decouples with the root zone with topographic position. As a result of this decoupling, there exists a seasonal hysteretic relationship between streamflow decay and both evapotranspiration and watershed wetness conditions. Results indicate that for portions of the year, forest transpiration may actively compete with subsurface drainage for the same water resource that supplies streamflow, though for extended time periods, these processes exploit distinct water stores. Our analysis raises concerns about the efficacy of assessing humid headwater systems using traditional recession analysis, with recession curve parameters treated as static features of the watershed, and we provide novel alternatives for evaluating interacting biological and geophysical drivers of streamflow recession.

KEYWORDS

headwater catchment, hysteresis, streamflow recession, transpiration, two water worlds

¹Department of Geological Sciences, University of North Carolina at Chapel Hill, Chapel Hill, North Carolina

²Department of Environmental Sciences, University of Virginia, Charlottesville, Virginia

³Department of Engineering Systems and Environment, University of Virginia, Charlottesville, Virginia

1 | INTRODUCTION

Hydrograph recession analysis relates the rate of streamflow decay to streamflow and is routinely performed to predict low flows, with implications for both water supply (Hornbeck, Adams, Corbett, Verry, & Lynch, 1993; Price, 2011) and habitat (Boulton, 2003; Konrad & Booth, 2005). It is also used (a) to derive master recession curves for use in some ecohydrological models (e.g., Neitsch, Arnold, Kiniry, & Williams, 2005), (b) to calculate total dynamic storage of a basin (e.g., Krakauer & Temimi, 2011), (c) to separate baseflow from streamflow (e.g., Eckhardt, 2005), and (d) to estimate basin-wide features such as average hydrological conductivity and aquifer depth (e.g., Rutledge & Mesko, 1996; Szilagyi, Parlange, & Albertson, 1998; Tague & Grant, 2004).

Brutsaert and Nieber (1977) proposed the following power-law model to describe recession by relating discharge (Q) to its time derivative $\binom{dQ}{dQ}$:

$$-\frac{dQ}{dt} = aQ^b. (1)$$

This novel conceptualization has several key features that have served subsequent research. Treating $\frac{dQ}{dt}$ as a function of Q eliminates the need for identifying a specific reference time for each recession event allowing objective and systematic analysis of recession curve characteristics for any gauged watershed and does not require an explicit estimate of storage or storage capacity. Further, the multiplicative factor (a) in Equation (1) reflects the integration of permanent basin-wide characteristics, whereas the exponent (b) describes temporal aquifer conditions. This widely used formulation also allows for both linear (b=1) and nonlinear $(b\neq 1)$ aquifer storage–discharge relationships.

Methods for conducting recession analysis (Tallaksen, 1995) and estimating a and b parameters (Equation (1)) have typically been performed by fitting models to recession flow data in one of three ways: (a) to a cloud of data points representing all recession events captured in a watershed (Krakauer & Temimi, 2011; Vogel & Kroll, 1992), (b) to the lower envelope of the data cloud (Brutsaert & Nieber, 1977), and (c) to the median values of binned data (Kirchner, 2009). These studies, with the exception of Kirchner (2009), assume recession that is solely a function of aquifer characteristics and is thus governed by fundamental groundwater hydraulics (Shaw & Riha, 2012). However, recession may not always represent deep aquifer conditions, particularly in regions where streamflow is predominantly fed by shallow subsurface aquifers. In these regions, storage and flow of water within the shallow subsurface can maintain flows for extended periods (Hewlett & Hibbert, 1967) facilitating interactions between active drainage and evapotranspiration (ET) that create diurnal (Bond, Jones, Phillips, Post, & McDonnell, 2002), seasonal (Shaw & Riha, 2012), and interannual (Sawaske & Freyberg, 2014) fluctuations in streamflow recession behaviour.

Recent studies have explored variation of recession behaviour by investigating individual recession events rather than point clouds (Bart & Hope, 2014; Biswal & Marani, 2010; Dralle, Karst, & Thompson,

2015; Shaw & Riha, 2012). Findings suggest that recession characteristics are linked to temporally variable catchment properties, such as rates of ET, antecedent wetness conditions (AWCs), or stream network contraction. Wittenberg and Sivapalan (1999) showed for a semiarid catchment in Western Australia that variation in *a* exhibited an annual sinusoidal pattern, peaking in summer and reaching a nadir in winter. They explained the seasonal oscillation of *a* as indicating a transition from relatively unstable streamflow in summer to relatively stable streamflow in winter as a consequence of competition with seasonal ET rates. This evidence provides some contrast to the two water worlds hypothesis (Berry et al., 2017; Brooks, Barnard, Coulombe, & McDonnell, 2010; Evaristo, Jasechko, & McDonnell, 2015).

Although numerous studies have shown that transpiration increases streamflow recession (e.g., Federer, 1973), more recent recession analyses that fit regressions to individual events have failed to detect a relationship between streamflow recession characteristics and transpiration (Biswal & Kumar, 2014; Shaw & Riha, 2012). The increase of a during the summer growing season (Dralle et al., 2015) has alternatively been ascribed to the depletion of groundwater and soil moisture, indicating that recession event behaviour is a function of both saturated and unsaturated zone storages (Bart & Hope, 2014: Shaw, 2016; Shaw & Riha, 2012). Therefore, previously observed relationships between ET and a values (Wittenberg & Sivapalan, 1999) may exist only because high rates of ET tend to drive down storage. However, when Biswal and Kumar (2014) directly investigated relationships between water table depth and a, they found no significant relationship for individual recession events in 34 basins across the United States.

Studies systematically analysing the effects of seasonality on event-based recession behaviour are limited (Tallaksen, 1995), contributing to a lack of consensus in findings (Dralle, Karst, & Thompson, 2016). Major impediments to the study of event-based recession behaviour are the mathematical anomalies that arise from the scalefree properties of power laws making the simultaneous independent treatment of the power-law variables, a and b, impossible. This has only recently been addressed in Dralle et al. (2015). Although the novelty of analysing individual recession curves as discrete, independent events is appealing, evaluating recession characteristics individual events becomes exceedingly difficult given complex hydroclimatological phenomena operating at many spatial and temporal scales and the lack of information on covarying transpiration rates and storage patterns. Studying specific drivers of recession curve characteristics requires continuous, long-term data collection (>10 years) that accurately represents variability of AWC, rates of ET, and stream network extent at several spatiotemporal scales. Collecting such long-term data can be costly and difficult. In particular, long-term watershed-level measures of available water content in the rooting zone, essential as a constraint on transpiration, are especially rare. Further, recession analyses are conducted using stream gage discharge data, which spatially and temporally integrate watershed-scale hydrological fluxes, further complicating efforts to isolate specific mechanisms contributing to recession behaviour. This top-down approach is useful for understanding long-term recession behaviour over large

spatial extents but may be inadequate on its own for developing a more process-based understanding of seasonal recession variability.

We explore the seasonal variability of recession curve characteristics in order to better understand the biophysical drivers of streamflow decay. Using long-term streamflow and soil moisture data from a forested headwater catchment in the southern Appalachian Mountains of North Carolina, USA, we describe empirical relationships among characteristics of event-based recession curves and seasonal patterns of ET and AWC using recently developed methods of recession analysis. We augment this analysis with watershed state and flux conditions computed using a process-based ecohydrologic model to directly incorporate ecosystem phenologic interactions and ET at a daily time step. We discuss the relationships between recession curve characteristics and estimates of ET, AWC, and stream network density and explore the physical and ecological processes governing these relationships using the Regional Hydro-Ecologic Simulation System (RHESSys).

Contrary to previous studies, we hypothesize that ET and AWC each independently affects patterns of streamflow recession and that the failure of previous studies to detect the influence of either (or both) is due to their seasonally dynamic covariance. Specifically, we hypothesize the following:

- 1 Fluctuations in watershed-scale AWC and rates of ET will each independently influence measures of streamflow recession.
- 2 Rates of ET will dominate streamflow recession behaviour in the early growing season, when ET is greatest and the groundwater table the highest, whereas AWC will dominate behaviour in the late growing season as groundwater levels decline and decouple with transpiration and in the nongrowing season when ET is minimal.

We discuss the implications of a temporally variable approach to recession analysis and the discovery of seasonally distinct recession curve patterns and present a process-based explanation of stream recessional behaviour that incorporates the shifting influence of ET and AWC at the annual and event scales.

2 | METHODS

2.1 | Study site

Recession analysis and modelling is conducted using data from the Coweeta Hydrologic Laboratory (CHL) located in the southern Appalachian Mountains in southwest North Carolina, USA (Figure 1; https://www.srs.fs.usda.gov/coweeta/tools-and-data/). CHL is a U.S. Forest Service site that is also part of the Long-Term Ecological Research network funded by the National Science Foundation. The Coweeta basin is drained by two main stems comprising a total drainage area 16.46 km² (Swank & Crossley, 1988). Relief from the valley floor to the ridge is roughly 1,000 m leading to a strong orographic effect that creates annual rainfall totals ranging from 1,700 mm at the base climate station to 2,500 mm at the highest elevation. Increasing hydroclimate variability in the region has manifested in more severe, prolonged droughts and greater rainfall in wet years (Ford, Hubbard, & Vose, 2011). The region has also experienced warming trends beginning between 1976 and 1981 at a rate of 0.5°C per decade (Ford et al., 2011).

Vegetation varies across relatively short elevation and moisture gradients at CHL ranging from xeric, low-elevation, ridge sites consisting of oak-pine forests, with more mesic canopy species in hollows and riparian zones, to northern hardwood forest in high-elevation, wet sites (Day & Monk, 1974). A dense evergreen understory of rhododendron (*Rhododendron maximum*) and mountain laurel (*Kalmia* sp.) exists in a significant portion of the basin (Day, Phillips, & Monk, 1988). In the last 10 years, growth of rhododendron has increased along stream corridors following extirpation of hemlock species by the hemlock woolly adelgid (Ford, Elliott, Clinton, Kloeppel, & Vose, 2012).

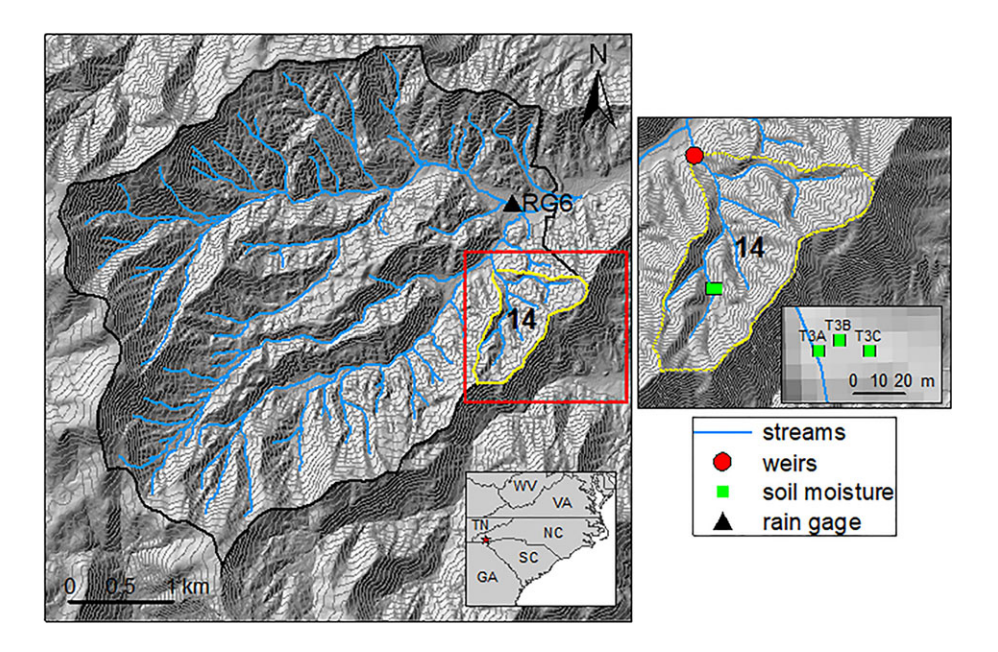


FIGURE 1 Study site map of the full Coweeta Hydrologic Lab and inset of watershed 14

Soils across CHL are well-drained sandy loams (Velbel, 1988) with a deep saprolite layer over folded schist and gneiss formations (Hatcher, 1988). Though no evidence of perched aquifers has been noted, the shallow subsurface sustains baseflow via unsaturated zone flow (Hewlett & Hibbert, 1963). Field observations indicate infiltration excess overland flow is rare or non-existent during even large, intense storm events and that stormflow is primarily associated with the expansion of the saturated variable source area (Hewlett & Hibbert, 1967).

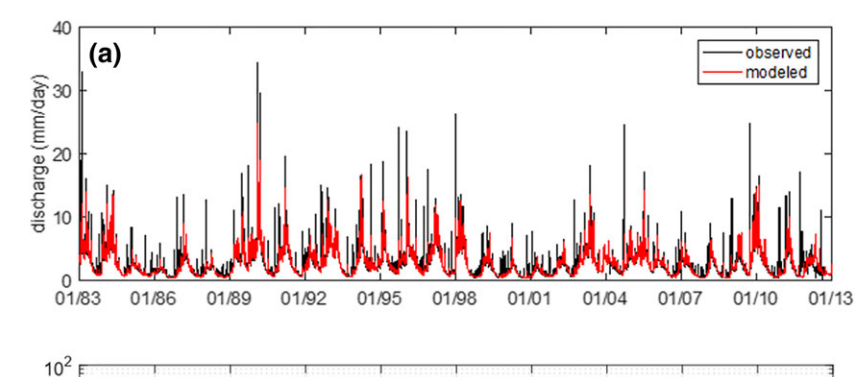
Our study focuses on watershed 14 (WS14), a low-elevation, northwest-facing catchment that has a drainage area of 0.62 km² (Figure 1). Vegetation is a mixed hardwood forest with 285-m relief. Rainfall data used in this study were collected at the base climate station (RG06; Figure 1), and due to the relatively small relief, orographic effects on rainfall are minor. Daily rainfall and temperature records have been collected since 1937 at the base climate station. Daily streamflow is also measured throughout CHL, with the earliest records beginning in the 1930s. In WS14 continuous daily streamflow was measured using v-notched weirs. We have limited our study period from 1983 to 2012 to capture the driest and wettest years on record and to reduce the time domain over which we model hydrologic behaviour.

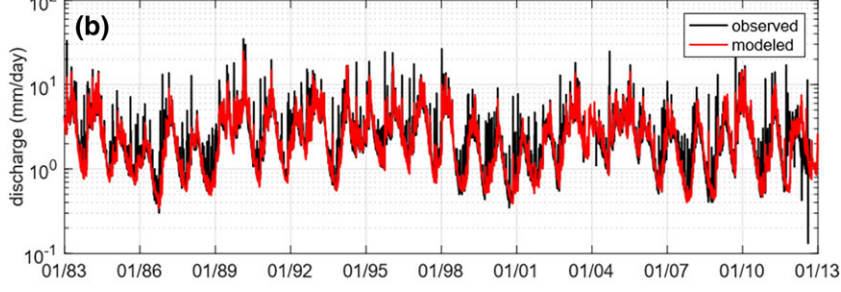
Observed AWC is estimated from CS616 time-domain reflectometry probes (Campbell Scientific, Inc., Logan, UT) that measure daily

soil moisture at three plots in our study watershed (Figure 1; https://coweeta.uga.edu/dbpublic/dataset_details.asp?accession = 4048). Each soil moisture plot consists of four buried time-domain reflectometry probes arranged in lower and upper locations of the plots and at two depths (0–30 and 30–60 cm). Continuous soil moisture is averaged across all four probes to estimate a mean soil moisture for the plot. We augmented our analysis by including measurements from a neighbouring watershed (WS18) because records there extend back to 1999, as opposed to 2011 at WS14. Because relative soil moisture readings in WS18 and WS14 rise and fall in concert, the analysis presented in this paper uses the longer term WS18 probes, and results from WS14 are provided in the supplemental material (Figures 2 and 3).

2.2 | Ecohydrologic modelling

To explore state and flux variables that contribute to event-based recession behaviour but are generally not observed, we use the distributed, process-based watershed model, RHESSys. RHESSys is a spatially explicit ecohydrological model that simulates coupled carbon, water, and nutrient cycling over a watershed (Band, Patterson, Nemani, & Running, 1993; Tague & Band, 2004). RHESSys is a fully distributed model simulating surface and subsurface hydrologic fluxes, including overland flow, return flow, shallow subsurface throughflow.





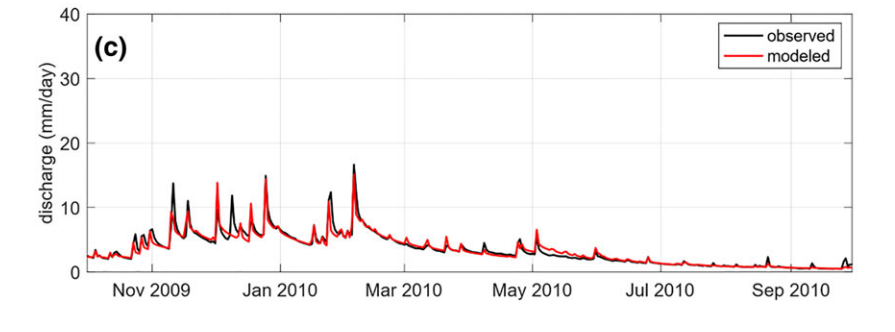


FIGURE 2 Hydrographs of model performance (red lines) against observed streamflow (black lines) for all years in the study on a (a) linear scale, (b) log scale, and (c) on a linear scale for a single representative water year

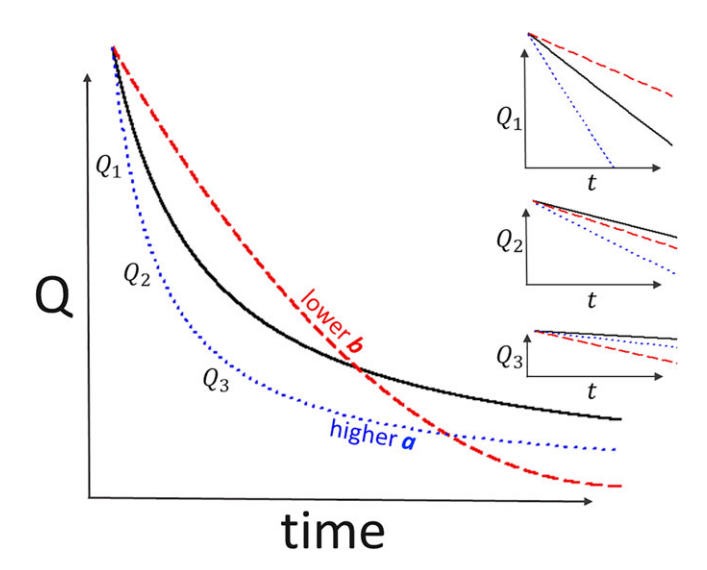


FIGURE 3 A representative hydrograph (solid black line) shown in relation to a hydrograph generated using a lower b value (dashed red line) and a higher a value (dotted blue line). The smaller plots in the top right illustrate the instantaneous slope of the hydrograph initiated at increasingly small values of *Q*

and deep groundwater flow. Return flow is calculated according to the Distributed Hydrology Soil Vegetation Model (Wigmosta, Vail, & Lettenmaier, 1994), a two-dimensional subsurface routing model with exponential decay of hydraulic conductivity with depth. Deep groundwater flow is calculated for the entire basin using a simple linear reservoir. Streamflow is estimated as the sum of these processes, as well as infiltration excess overland flow during periods of rainfall. State variables such as subsurface storage and groundwater levels are updated and stored at daily time steps. We used groundwater levels to characterize modelled AWCs. Evaporation and transpiration are simulated using the Penman–Monteith equation, with a stomatal physiology parameterized with locally available data.

The model is calibrated for WS14 with groundwater parameters that represent flow from deep aquifers to the stream constrained to a low fraction of total flow because streamflow at CHL is thought to be predominantly shallow subsurface (Hewlett & Hibbert, 1967). We computed a Nash-Sutcliffe efficiency value of 0.755 from the calibrated constrained model and the observed flow over the study period (1983–2012), and a Nash-Sutcliffe efficiency value for log(Q) of 0.845.

2.3 | Estimation methods for power function parameters

Recently, Dralle et al. (2015) described how mathematical anomalies that arise from the scale-free properties of power laws may interfere with standard approaches to recession analysis. Some previous studies have attempted to resolve this issue by holding b constant and evaluating relative changes in a, whereas others have allowed both a and b to vary but exclusively analysed changes in the value of b (e.g., Biswal & Marani, 2010; Biswal & Kumar, 2014; McMillan et al., 2014;

Stoelzle, Stahl, & Weiler, 2013; Tague & Grant, 2004). Whereas the latter approach precludes analysis of fitted values of a, the former precludes analysis of b and introduces bias in the values of a. To allow analysis of the relationships between physical processes and both b and a with minimal bias, we used the methods described by Dralle et al. (2015).

2.4 | Recession analysis

There is no standard method for identifying periods of recession, especially in the relatively novel subfield of recession analysis of individual events. We relied on Dralle, Karst, Charalampous, Veenstra, and Thompson (2017), who recently assessed methodological uncertainty among different selection procedures and ultimately recommended simple and commonly used selection criteria, such that recession must have (a) decreasing streamflow and (b) decreasing streamflow derivatives for at least four consecutive days. That is, both O and – dO/dt must decrease for at least four days. Recession events continue until either of these conditions are violated. Stoelzle et al. (2013) showed that criteria for selecting periods of recession had a moderate impact on the values of a and b when performing recession analysis on data point clouds. To remove the possible effects of stormflow, which typically occur during and immediately after storm events, we eliminated the first day of each recession event before analysis. Previous studies removed several days, or weeks, of streamflow data following peak flow. However, the deep, highly conductive soils at CHL allow nearly instantaneous infiltration of rainfall resulting in negligible infiltration excess overland flow even during high intensity summer thunderstorms. Although saturation excess overland flow and return flow are noted in the watershed, such flow is localized, occurring over short lengths and times, such that recession is dominated by discharge to the stream network from the subsurface. The exceptionally humid climate, smaller catchment size, lack of snowpack, and evenly distributed annual rainfall make streamflow recession short lived at WS14, in comparison to other studies that may be snowmelt dominated (Tague & Grant, 2004) or have Mediterranean climates. Interstorm periods last, on average, 4 days at Coweeta, but have surpassed 60 days during severe drought.

After decorrelating each data set (Figure S1), we determined values of *a* and *b* for each recession event using measured and modelled discharge (Figure 4). Values of *a* and *b* were summarized by month and season and compared with those values computed from linear models fit through the entire point cloud. Stoelzle et al. (2013) showed markedly different *a* and *b* values based on whether models were fit using all sampling days (Vogel & Kroll, 1992), just days comprising the lower envelope of the point cloud (Brutsaert & Nieber, 1977), or the central tendency of the point cloud (Kirchner, 2009). However, while we applied each procedure to our analysis of the data in aggregate, we determined that only the fitting procedure of Vogel and Kroll (1992) could be consistently applied to event data, for which there are typically fewer than 10 data points per event.

A practical illustration of the effects streamflow recession variables have on the hydrograph is provided in Figure 3. An increase in

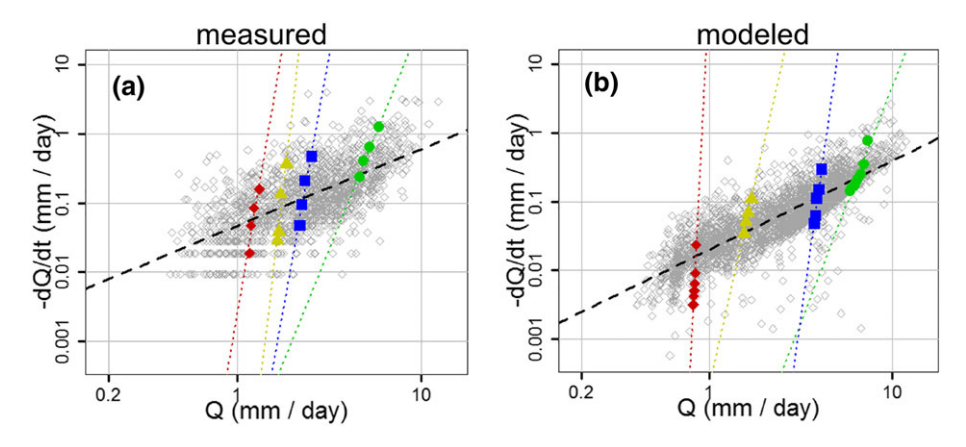


FIGURE 4 Recession curves of (a) measured and (b) modelled streamflow at the Coweeta Hydrologic Laboratory. Black dashed lines represent recession curves generated by linear model of all point cloud data. Red diamonds, yellow triangles, blue squares, and green circles are illustrative of the daily Q and dQ/dt values of individual recession events randomly chosen during the fall, summer, winter, and spring (respectively), whereas the coloured dotted lines represent models for each event. Note that the individual events selected are representative of recession behaviour, but measured and modelled results are not coincident

the value of a increases rates of streamflow "decay." The value of b is a measure of "nonlinearity," with greater nonlinearity enhancing the concavity of the hydrograph, though the instantaneous slope of the hydrograph is dependent on the actual rate of streamflow. Increasing the value of b results in streamflow receding more quickly during periods of high streamflow and becoming more stable during periods of low streamflow.

3 | RESULTS

3.1 | Observed recession behaviour

We identified 382 recession events using observed data. Log-log plots of Q to $\frac{dQ}{dt}$ were fit for both observed and simulated streamflow with linear models for each individual recession event, which yielded a wide range of b values (from Equation (1)) spanning two orders of magnitude. The typical b value of individual recession events ranged between 4 and 20 with a median value of around 11, much higher (i.e., a steeper recession slope) than those computed by fitting a model to the entire data cloud or with respect to seasonal data clouds that were between 1 and 1.5 (Figure 5). Regression models of individual recession events also generated $\log(a)$ values spanning two orders of

magnitude, with typical log(a) values of around -12 compared with log(a) values generated by linear models of the entire and seasonal point clouds ranging from -3 to -5 (Figure 5).

At WS14, monthly streamflow was highest in March and lowest in September. To assess similar seasonality in recession characteristics we plotted logs(a) and b values for each event by day of year and summarized typical values by month using box and whisker plots (Figure 6). Values of log(a) formed a sinusoidal pattern, with values tending to increase (i.e., greater streamflow decay) from spring to summer and to decrease (i.e., more stable streamflow) from summer to winter. Specifically, median log(a) reached a minimum in April, lagging the annual streamflow maximum by a month, and peaking in September, in concert with annual streamflow minimum. The range of monthly log(a) values also exhibited seasonality, with greater variability in the winter months and less after April. Values of b exhibited a weaker pattern, generally increasing from May to October and decaying to a minimum in March, though relatively elevated b values in month of April interrupted an otherwise sinusoidal pattern.

We explored the possible effects of potential ET (PET), computed using the Penman–Monteith equation with observed atmospheric data, on recession characteristics. Viewing the data in aggregate reveals no immediately evident relationships between either logs(a) or

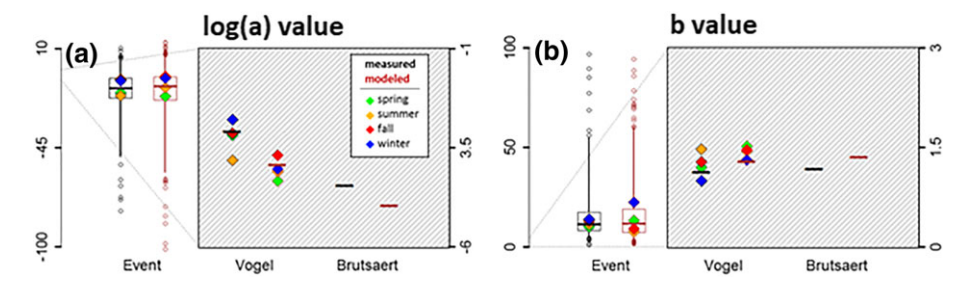
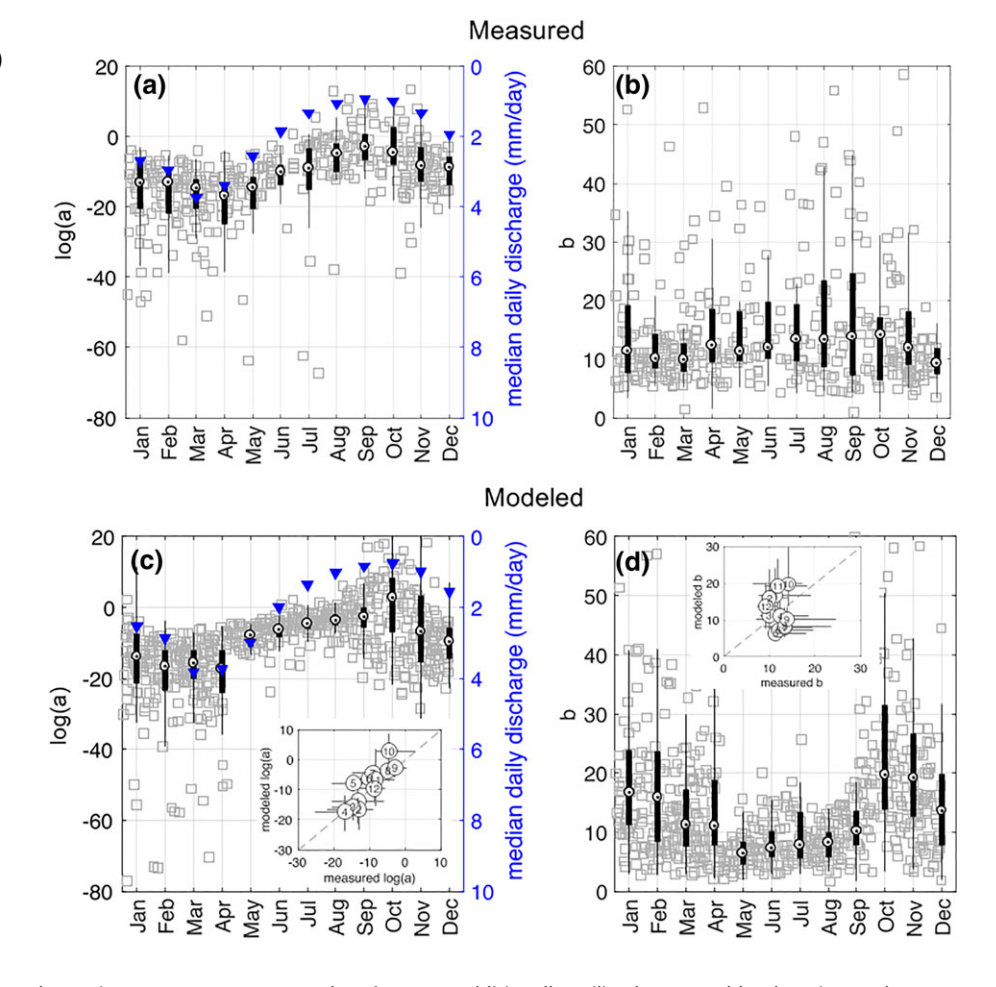


FIGURE 5 Measured (black) and modelled (brown) values of logs(a) (left) and b (right) for spring (green), summer (orange), fall (red), and winter (blue). For event data, the box represents 50% of data and whiskers 90% of data, whereas the diamonds represent seasonal median values. Note that the y-axis on the left of each plot indicates values for events, whereas the y-axis on the right of each plot indicates values generated using a linear model of the point cloud (Vogel) or of the lower envelope of the point cloud (Brutsaert)

FIGURE 6 Seasonal variations in logs(a) (left) and b (right) of measured (top) and modelled (bottom) streamflow. Small grey squares indicate values for individual events by day of year. Median values, 25th to 75th percentile, and 5th to 95th percentile of binned monthly values are represented by black dot, thick black bar, and thin black bar, respectively. Median daily streamflow values by month are shown by blue triangles. Insets show modelled monthly values of logs(a) (left) and b (right) plotted against measured values, with a dashed one-to-one line



b and PET (Figure 7). Unsaturated zone volumetric water content (VMC) estimated using long-term continuous soil moisture measurements are poorly correlated with b and negatively correlated with $\log(a)$, indicating that drier soils generate greater streamflow decay.

Summarizing the data by median monthly values to examine seasonal variation revealed strong counterclockwise hysteresis in plots of log(a) and PET (Figure 7). Log(a) values were depressed during the transition from winter to spring, as PET rates rose. Rates of PET peaked in midsummer, whereas log(a) values continually increased into the late growing season. Finally, from September to December, PET rates plummeted, and log(a) values decreased gradually. Plots of log(a) against VMC hinted at hysteresis but in the clockwise direction, with no hysteresis evident in the midsummer. The timing of shifts does not explain our observations in log(a)-PET relationships. Periods during summer and winter when log(a)-PET relationships shift between high and low log(a) values without commensurate shifts in PET were not concurrent with shifts in log(a) to VMC, which may indicate processes other than PET and VMC driving recession characteristics. b was poorly correlated with PET and negatively correlated with b with no discernible hysteretic loop.

Estimates of VMC computed using soil moisture measurements neglect both deep unsaturated soils and all saturated zone dynamics when soil saturation levels are below 60 cm. To thoroughly assess the relationships between recession characteristics computed from observed discharge and AWC in both the unsaturated and saturated

subsurface, we additionally utilized water table elevation and extent of saturated area derived from the RHESSys model (Figure 8). We also analysed the relationship between recession characteristics and transpiration derived from RHESSys (Figure 8) because estimates of PET computed using Penman-Monteith are primarily temperature driven and do not accurately capture phenology, soil moisture signals in transpiration signals. Log(a) was negatively correlated with both water table elevation and saturated area. b was poorly correlated, though there was possible counterclockwise hysteresis in its relationship with both water table elevation and saturated area variables. Modelled transpiration and log(a) demonstrated counterclockwise hysteresis similar to PET, though it was apparently uncorrelated with b. Patterns of modelled transpiration better represent seasonal controls that phenology exhibits on log(a) values. During the dormant season between November and April, transpiration is near zero, and it exhibits the strongest controls on recession following leaf out when rates are increasing.

3.2 | Modelled recession behaviour

Using the discharge generated from RHESSys, we identified 641 recession events and conducted identical recession analyses. We found that typical values of logs(a) and b derived from model output generally agreed with those derived from observations as shown in Figures 5 and 6. The range, median value, and variability of log(a) and

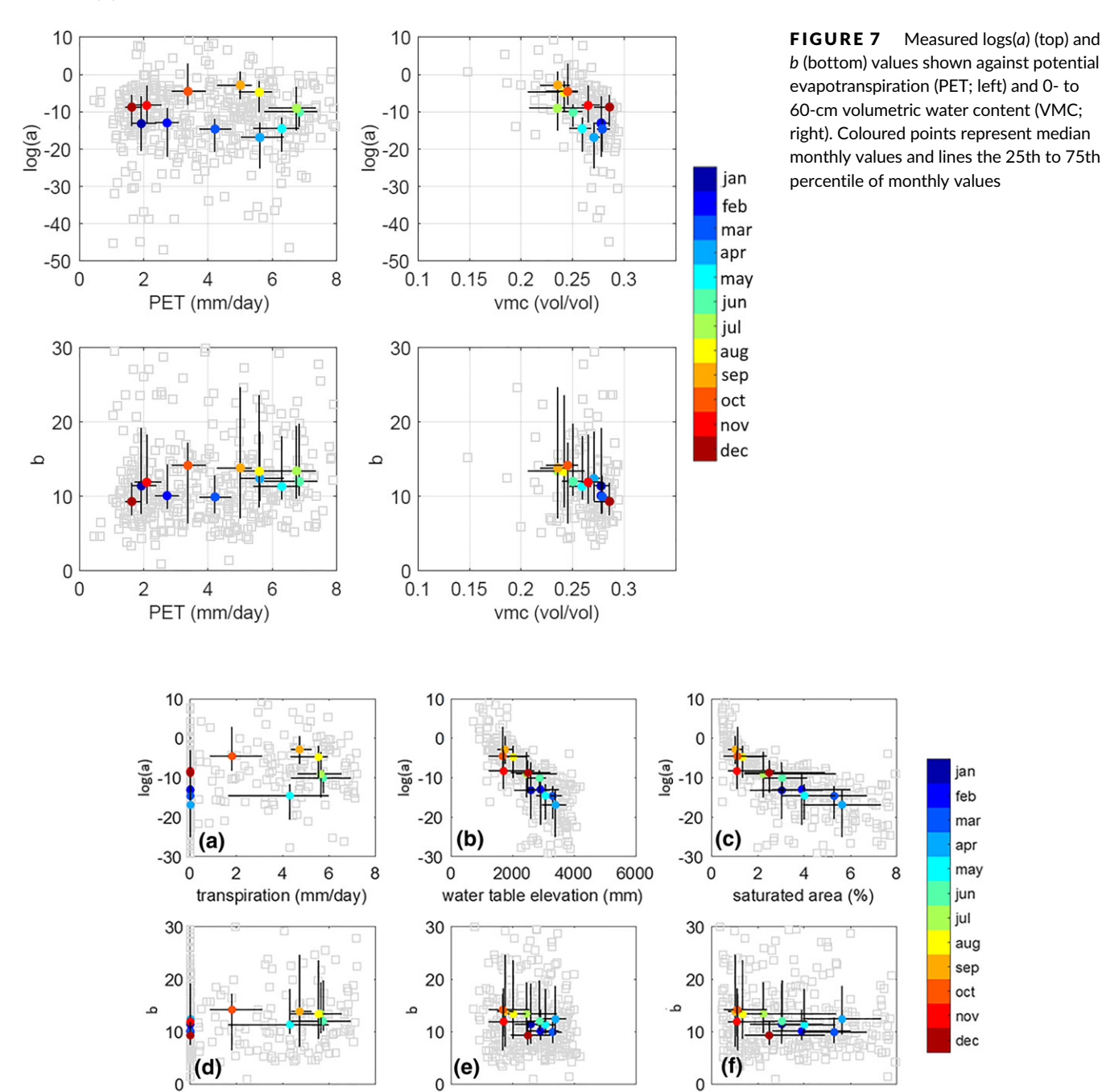


FIGURE 8 Measured logs(*a*) (top) and *b* (bottom) values shown against modelled transpiration (left), water table elevation (middle), and watershed percent saturated area (right). Coloured points represent median monthly values and lines the 25th to 75th percentile of monthly values

water table elevation (mm)

saturated area (%)

b values from the observed record is consistent with modelled results (Figure 5). Overall, annual patterns of log(a) matched those from the observed data set, increasing from April to September in the observed data set and April to October in the modelled data set then declining until April in both cases (Figure 6). The model underpredicted b values and the variability of those values in the growing season from May to late September and slightly overpredicted b variability in the dormant season from October to April. Although modelled monthly values of log(a) accurately predicted measured monthly values with little bias,

transpiration (mm/day)

the relationship between modelled monthly values of b and measured results was more complicated (Figure 6). Two distinct trends are evident, with b values from both the model and the observed record decaying in the nongrowing season and increasing during the growing season, with modelled b values peaking in October (coincident with measured results) and decaying until May (lagging measured results by 2 months). Yet the modelled values of b were generally depressed during the growing season as a whole. It was not apparent if the seasonal pattern in values of b is muted in the observed record due to a

less robust data set and potential measurement error or if the model overestimated the seasonality of *b* values and lag time between a transpiration shift and baseflow response.

In Figure 9, $\log(a)$ computed from modelled discharge is poorly correlated with transpiration but illustrates well-defined counterclockwise hysteresis, as was also shown with observed data. Starting in April, transpiration rates quickly increased peaking in June, and $\log(a)$ values increased slightly above median annual values of -11 (Figure 9). From June to October, transpiration begins decreasing as $\log(a)$ values continued to rise. Patterns of b values with transpiration were also similar to our measured data demonstrating a counterclockwise hysteretic loop. However, viewed in aggregate, the modelled values of b had a general negative trend, whereas observed b values exhibited no apparent trend with transpiration. This sensitivity of modelled b values to transpiration is a likely cause of the underprediction of b values during the growing season.

Log(a) is negatively correlated with both water table elevation and saturated area. b values, though, show no general trend with either water table elevation or saturated area when data is viewed in aggregate. However, b decays with an increase in either wetness condition variable during dry down (May to September) or wet up (October to April). The apparent lack of a relationship between b and watershed moisture is caused by the stark shift in b values during seasonal dry down and wet up.

Finally, we assessed seasonal variability in the strength of the relationship between $\log(a)$ and both water table elevation and transpiration. We binned all 641 recession events by month, with each month capturing at least 40 events. We predicted $\log(a)$ with water table elevation and transpiration using a linear model and described the strength of that relationship according to the r^2 value (Figure 10). Correlation was highly seasonal. Water table elevation tightly constrained values of $\log(a)$ from July to November with r^2 values greater.5, with

the exception of October. From December to June, variance increased, reducing correlation. Transpiration showed the highest correlation with log(a) in May to June and was completely uncorrelated by August.

4 | DISCUSSION

4.1 | Event-based versus point cloud recession characteristics

Recession analysis performed using individual events generates strikingly different recession parameters than are generated using point

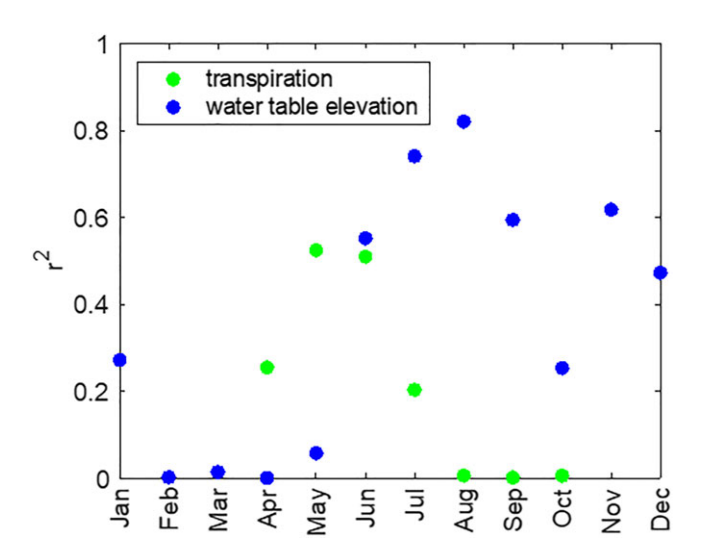


FIGURE 10 r^2 value of a linear model relating monthly values of modelled log(a) to water table elevation (blue squares) and to transpiration (green circles)

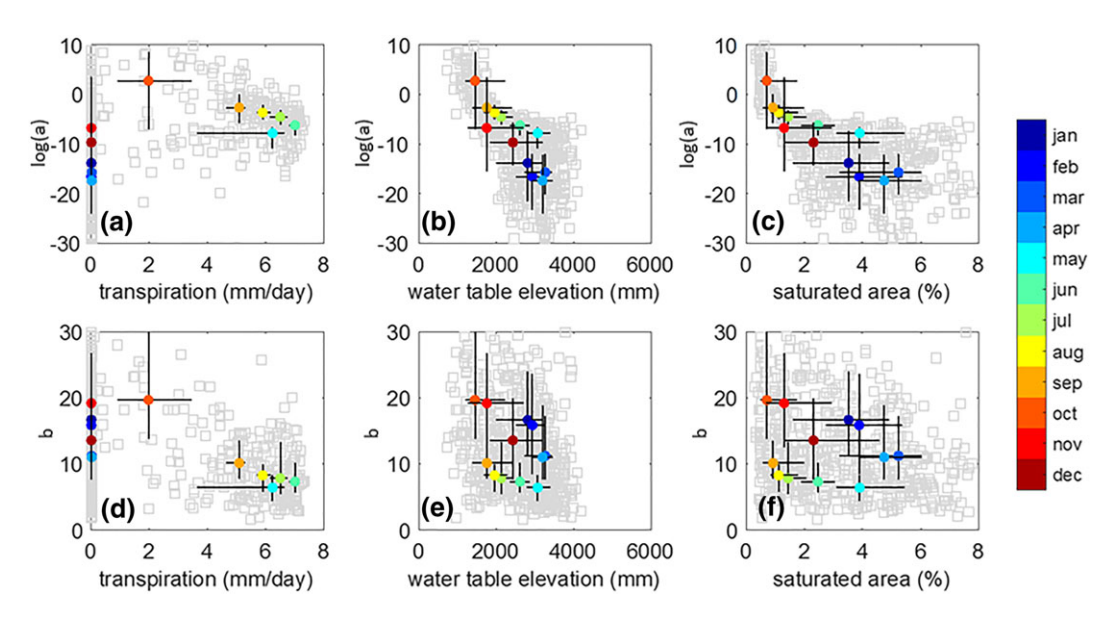


FIGURE 9 Modelled logs(*a*) (top) and *b* (bottom) values shown against modelled transpiration (left), water table elevation (middle), and watershed percent saturated area (right). Coloured points represent median monthly values and lines the 25th to 75th percentile of monthly value

cloud data, as shown in the previous studies (e.g., Shaw & Riha, 2012). Traditionally, the lower envelope of points in a data cloud is seen to represent the time periods when streamflow is entirely dependent on deep groundwater stores (Tallaksen, 1995). During periods when streamflow is entirely fed by deep groundwater, recession events are expected to follow this lower envelope, predicted to have a b value of 1 or 1.5 (Brutsaert & Nieber, 1977), as has been validated empirically (e.g., Vogel & Kroll, 1992). If the nonlinearity of the observed recession curves decreased as streamflow decayed, as predicted by outflow from a Boussinesq aquifer, we would expect the curve of individual recession events to exhibit a concave pattern (McMillan, Clark, Bowden, Duncan, & Woods, 2010). However, the individual recession slopes in our study tend to be convex. Also, the lower envelope in our analysis is comprised almost exclusively of only the final day(s) of individual recession events whose slopes are generally much greater than 1.5. Therefore, at CHL, the slope of the lower envelope of the entire point cloud does not reflect the instantaneous state of the aguifer. Instead, the slope of the lower envelope may be interpreted as a signal of seasonal shifts in transient watershed features driven by other processes, such as rates of transpiration, AWCs, or stream network connectivity.

Equation (1) is often solved to determine watershed properties, where a is a function of the hydraulic properties and physical dimensions of the watershed (Brutsaert & Nieber, 1977; Rutledge & Mesko, 1996; Szilagyi et al., 1998). However, Troch, De Troch, and Brutsaert (1993) showed that estimates of hydrological conductivity using a values derived from point cloud regression or the lower envelope of the point cloud were up to one hundred times greater than estimates from laboratory measurements on soil samples. Furthermore, our results confirm recent findings that a is highly variable between recession events and strongly affected by seasonality (Dralle et al., 2015; Shaw & Riha, 2012). Thus, values of a at CHL are not only wholly dependent on static watershed properties like geophysical characteristics or deep aquifer hydraulic properties but also determined by more transient processes.

Although recession parameters are commonly used to predict low flow dynamics, comparison of parameter values derived using point cloud data with the median values of individual events at CHL shows typical values of log(a) are four times lower and values of b are an order of magnitude higher for individual recession events. Therefore, use of a master recession curve generated from a point cloud, as is common practice, may tend to systematically overestimate streamflow decay and underestimate streamflow nonlinearity, leading to underestimates of total streamflow during extended periods of low flow at CHL. Complex, nonstationary flux relationships that are commonly noted in empirical studies (e.g., Tashie, Mirus, & Pavelsky, 2016) may serve as significant buffers (or intensifiers) of climate and land use driven watershed dynamics and therefore should be integrated into predicative modelling efforts.

Interestingly, although modelled results generate slightly higher typical log(a) values for individual events than do measured streamflow data, they generate lower log(a) values for point cloud data than do measured streamflow data (Figure 5). This holds true

whether data are viewed in aggregate or disaggregated by season and whether point cloud data are assessed using the methods of Vogel and Kroll (1992) or Brutsaert and Nieber (1977). Thus, the model is effectively underestimating streamflow decay across the seasons, while overestimating the decay of streamflow during individual events. If point cloud-derived *a* values are indicative of unexplored seasonal dynamics, the model may have been calibrated to overestimate the decay-related parameters (e.g., increase transmissivity or decrease soil thickness) to compensate for a limited ability to mimic this seasonal increase in streamflow decay.

4.2 | Consistency in b values

In our results, the data point cloud of both observed and modelled streamflow generates slopes between 1 and 1.5, values that agree with the results of previous studies (e.g., Vogel & Kroll, 1992). However, the slopes of the individual recession events identified in this study are much steeper than identified in most previous studies, with a median value of around 11 as compared with around 2 or 3 in most previous studies (e.g., Biswal & Kumar, 2014; Shaw & Riha, 2012). Many studies have focused on watersheds with physio-climactic characteristics dissimilar to those at CHL: Shaw and Riha (2012) limited their study to seven medium and large basins (100-6,415 km²) in upstate New York; and Dralle et al. (2015) to 16 medium to large (33.9-1,929.5 km²) seasonally dry basins in the Pacific Northwest. However, several studies have included representative watersheds from across the continental United States: Biswal and Marani (2010) and Biswal and Kumar (2014) each included basins from across the continental United States (35 basins from 150 to 759 km² and 67 basins from 9.6 to 8,858 km², respectively). Therefore, it is unlikely that physio-climatic factors solely drive this discrepancy.

Interestingly, a series of studies in a similarly small (0.41 km²), humid (1,220-mm rainfall), forested headwater catchment at the Panola Mountain Research Watershed in Georgia, USA, arrived at recession characteristics which are strikingly similar to our results from nearby CHL: recession nonlinearity increases with time (i.e., a convex recession curve; Clark et al., 2009; Wang, 2011; and Ghosh, Wang, & Zhu, 2016), and late stage b values range from 4.3 to 29.4, with a median value of around 9 (Ghosh et al., 2016). Using 5-min interval discharge data and coincident observations of the wetted stream network, Ghosh et al. (2016) showed that early stage recession behaviour was dominated by the contraction of ephemeral streams, whereas late stage recession was dominated by decreasing subsurface discharge to perennial streams. However, our results from RHESSys show the extension of the stream network as a muted response to the elevation of the water table, not as a temporal driver of recession at WS14. Alternatively, Clark et al. (2009) used parallel aquifers to accurately describe this behaviour, with parallel aguifers being the manifestation of between-hillslope heterogeneity, whereas Wang (2011) relied on hillslope bedrock leakage and return flow. RHESSys incorporates each of these processes, with a deep linear reservoir fed by hillslope leakage and exfiltration directly from hillslopes of varying hydrologic properties. A complicating factor is that both Clark et al.

(2009) and Wang (2011) showed that recession at the hyper-local scale (i.e., a 0.1-ha hillslope) behaved like a linear reservoir and that the nonlinearity of individual events actually increased with scale. A potential explanation is that a single hillslope may behave like a Boussinesq aquifer, whereas heterogeneity among hillslopes or between the near subsurface and deep surface may drive nonlinearity at the scale of a headwater catchment, as shown at CHL and Panola. As scale increases, the number of heterogeneous processes contributing to streamflow multiply, muting the distinctiveness of the contribution of each, and thereby driving nonlinearity back down, as seems to be the case in most previous studies in larger basins. Future investigations into potential relationships between basin scale and the nonlinearity of individual recession events may prove fruitful.

4.3 | Dual drivers of recession: Transpiration and wetness conditions

It has been well-established that transpiration directly and indirectly affects streamflow recession (Federer, 1973; Wondzell, Gooseff, & McGlynn, 2007). Bond et al. (2002) showed that diel pumping due to transpiration produced noticeable fluctuations in baseflow in their study in Watershed 1 at the HJ Andrews Experimental Forest. The diel pumping signal in baseflow diminished into the late growing season implying decoupling between the root zone and regions where baseflow is generated. Scaife and Band (2017) similarly hypothesized that transpiration can compete with active drainage in the root zone in recessional stormflow producing different stormflow hydrographs. Yet some recent research attempting to link transpiration rates to streamflow recession using seasonal variations in recession parameters has failed to find a significant correlation (Biswal & Kumar, 2014; Shaw & Riha, 2012). Our discovery of hysteresis in the relationship between streamflow recession parameters and rates of transpiration indicates a potential switching in the processes governing streamflow recession, both helping to confirm transpiration as a driver of streamflow recession and illuminating a factor potentially obfuscating the identification of this relationship.

Like Bond et al. (2002), we found that early growing season transpiration rates were correlated with streamflow recession characteristics (Figure 10). At CHL, the onset of the growing season occurs in early May in low-elevation north-facing catchments (Hwang, Song, Vose, & Band, 2011), which coincided with a rapid increase in correlation between log(a) values and modelled transpiration rates during May and June as shown in Figure 10. The influence of transpiration on streamflow recession continued with increasing PET until August, when it faded as shown by its decorrelation from log(a). Variation in log(a) shifted from dominance by transpiration to water table elevation later in the growing season and into the dormant season. This implies that as the season progresses into late summer when the depth of lateral subsurface flux drops below the rooting zone and recharge from the shallow unsaturated zone decreases, transpiration becomes decoupled from the shallow subsurface drainage that is hypothesized to produce baseflow following Hewlett and Hibbert (1967). This decoupling depresses transpiration signals in streamflow recession. When data are viewed in aggregate irrespective of month, the signal is difficult, if not impossible, to distinguish. We suggest that previous studies investigating controls of transpiration on recession characteristics may display similar hysteresis and decoupling when seasonality of transpiration and watershed wetness is considered.

This seasonal decoupling has intriguing implications suggesting temporality for the two water worlds hypothesis (McDonnell, 2014) in humid, temperate systems. The two water worlds hypothesis describes soil water used for ET ("green water") and groundwater that supplies streamflow ("blue water") as isotopically distinct sources (Evaristo et al., 2015). At CHL, where the water table and soil moisture levels are generally high, there exists a narrow timeframe (May and June) when transpiration is seen to compete directly and significantly with subsurface drainage that supplies streamflow. During this brief period from May to June, sources of green and blue water may interact to influence streamflow recession. Our findings suggest that the two water worlds hypothesis may hold true when transpiration is depressed (fall and winter) or when the shallow subsurface is too dry to sustain streamflow (summer) but breaks down under wet subsurface conditions and high transpiration rates characteristic of the early growing season. This hypothesis is consistent with the plotting position of CHL (North Carolina, USA) in figure 2 of Evaristo et al. (2015), and it may be further investigated with long-term isotopic data (Berry et al., 2017).

The relationship between groundwater storage and streamflow recession is axiomatic but complex. Higher water tables are associated with greater baseflows, which tend to result in lower a values and decreased streamflow decay as seen in Figure 9. This inverse relationship is similar to observations by Wittenberg and Sivapalan (1999). In their study, they computed a storage factor, similar to our measure of shallow groundwater level, and found that this storage factor decreased during the summer and increased during the winter months creating a transition from unstable to stable streamflow recession, respectively. We provide the additional observation that patterns of groundwater levels also show counterclockwise hysteresis with log(a) and clockwise hysteresis with b during the transition from spring to fall, with higher logs(a) and lower b values than the transition from fall to spring (Figure 8 and 9). Higher log(a) values during the spring to fall transition signify relatively greater streamflow decay for equivalent groundwater levels. Lower b values during this period signify decreased nonlinearity or a more consistent decline in streamflow. This observation, enhanced in the modelled results (Figure 9), suggests that although groundwater levels are a primary constraint on streamflow and streamflow recession, their influence is strongly affected by growing season water use due to transpiration removing actively draining water in the rooting zone.

4.4 | Circles within circles: More hysteresis

Correlation between log(a) and groundwater levels does not explain the late growing and dormant season recession characteristics entirely. In Figure 9, between February and May, the relationship between log(a) and water table elevation breaks down resulting in r^2 values below.1. During this period of time, median monthly b also decreases dramatically from 16 to 6 (Figure 6). Although the decorrelation method described above does remove any relationship between logs(a) and b when viewed in aggregate, analysing the decorrelated recession characteristics by month reveals more seasonally defined hysteresis loops (Figure S1). Log(a) increases from April to October and decreases from October to February, and b decreases from October to May and increases from May to October. The sharp rise in log(a) between April and May indicates increased streamflow decay due to the initiation of transpiration, which increases more gradually as soil moisture and groundwater are consumed. Log(a) then gradually decreases as soil moisture and groundwater levels recover. The rise in b from May to October indicates increased nonlinearity, as the shallow subsurface is drained of water and streamflow becomes increasingly dependent on deeper groundwater stores and transient soil moisture from precipitation events. Nonlinearity decreases as the watershed is rewetted during the dormant season, reaching a minimum during the initiation of transpiration. Thus, the period of wet up drives down streamflow decay and drives up nonlinearity, whereas the period of dry down drives up streamflow decay and drives down nonlinearity. This may be due to transmissivity feedbacks, as well as wetter soils facilitating stream network expansion, thereby decreasing the flow distance to the nearest actively flowing stream.

If shifts in logs(a) and b represent systematic responses to transient features of the landscape, one would expect to see hysteretic relationships between several other transient watershed features. For example, the results of our model show that the percentage of saturated area, an indicator of the transient expansion of the stream network, increases with water table elevation but is substantially lower during periods of dry down than wet up given the same water table elevation. Similarly, Godsey and Kirchner (2014) observed a seasonal shift in the relationship between catchment discharge and drainage density, with drainage densities being higher in the summer than the

winter during periods of similar flow volumes. Taking into account the hysteretic nature of these types of relationships is essential to developing a nuanced understanding of the fundamental processes governing streamflow.

4.5 | A biophysically based explanation of results

These results imply that in CHL, transpiration and subsurface conditions work in concert to generate seasonally distinct patterns of streamflow recession (Figure 11). In March to April, after wet up, the water table is at its highest level; streamflow decay is at a minimum, and nonlinearity is moderate (Figure 11a). Then, in May, the deciduous overstorey begins transpiring, consuming water in the shallow subsurface (Figure 11b). Because the water table is high and the shallow unsaturated zone is wet in early spring, shallow water that would otherwise generate streamflow is partially consumed by transpiration, lowering rates of streamflow immediately. Concurrently, streamflow decay and nonlinearity increase as transpiration consumes water from the highly transmissive shallow subsurface that would otherwise contribute to streamflow. As the season progresses and transpiration drains the shallow subsurface in the hillslopes, transpiration decouples from mobile water stores and no longer impacts streamflow directly (Figure 11c). Although vegetation in hollows and riparian areas will continue to directly compete for mobile water, the relative extent of these zones diminishes through the growing season. For an increasing proportion of the watershed, diminished levels of transpiration depend on root zone soil moisture that is replenished by frequent rainfall but have limited direct influence on streamflow due to a decoupling of blue and green water stores.

Following leaf off in early fall, watershed moisture levels begin to recover, and streamflow increases commensurately (Figure 11d). Deep groundwater stores recharge slowly, whereas the shallow, highly transmissive unsaturated zone is replenished immediately by

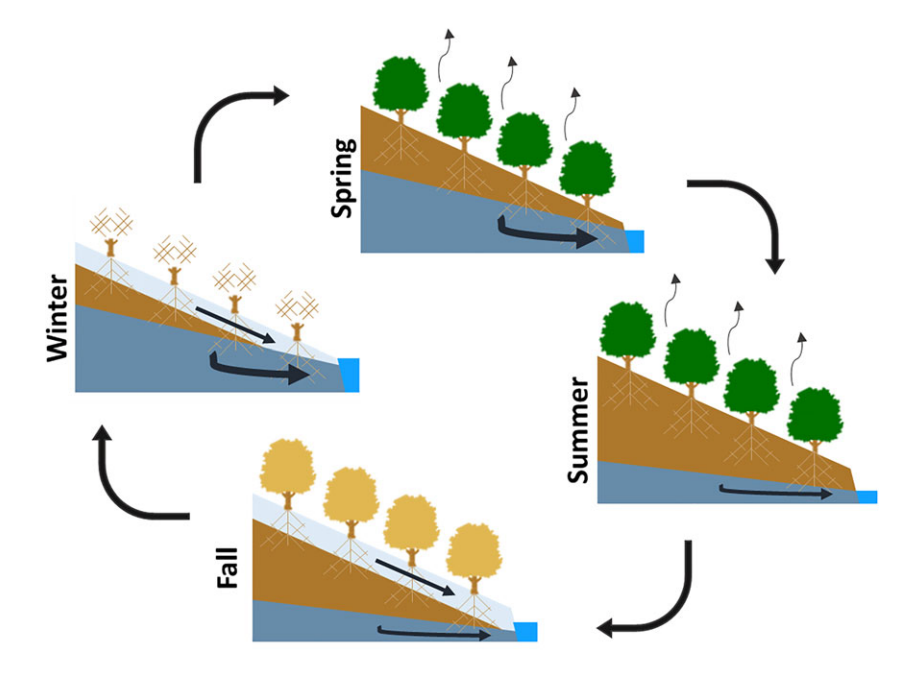


FIGURE 11 Conceptual model of seasonal dynamics governing streamflow dynamics at the Coweeta Hydrologic Laboratory: (a) highest streamflows, minimum decay, and moderate nonlinearity occur in late winter when both high water tables and shallow unsaturated zone throughflow generate discharge; (b) streamflow and nonlinearity decrease and decay increases as ET drains the unsaturated zone in spring; (c) streamflow decreases and decay and nonlinearity increase through summer, as the water table drops and evapotranspiration prevents recharge; (d) streamflow increases, decay decreases, and nonlinearity maximizes as a recharged shallow unsaturated zone supplements depleted deep groundwater contributions to streamflow; (a) streamflow increases and decay and nonlinearity decrease as the water table is replenished

precipitation events and then quickly drains, with baseflow becoming more dependent on deeper stores. Therefore, in the early winter after leaf off, streamflow nonlinearity is highest, with streamflow decaying quickly to a stable low flow regime, as the shallow unsaturated zone is quickly drained and flow becomes dependent on deep storage. As the water table rises over the winter, streamflow becomes ever less dependent on shallow storage, whereas average aquifer transmissivity and stream network density increases. Therefore, typical streamflow values increase; streamflow decay plummets, and nonlinearity steadily diminishes. This process continues until leaf on in early spring, when the cycle repeats itself.

It is important to note that this final analysis proceeds primarily from evaluation of modelled catchment behaviour. Although the model does accurately represent streamflow (Figure 2), average values of logs(a) and b (Figure 5), and seasonal patterns of log(a) (Figure 6), it likely exaggerates dynamics in values of b (Figure 6). If time-varying contributions to streamflow by the near and deep subsurface are the appropriate mechanism for describing dynamics in nonlinearity at Coweeta, then the simplifying assumptions underlying RHESSys streamflow present a likely explanation. Specifically, flow in the near subsurface is explicitly routed and serves as a potential source of transpiration, although deep groundwater is modelled according to a lumped linear reservoir below the root zone. With leaf on in May, the highly variable moisture in the root zone is largely consumed by transpiration, whereas less variable stores of groundwater continue to discharge to the stream network unimpeded, thus constraining the variability in values of both logs(a) and b (Figure 6). A more moderate response is likely in actual watersheds where discharge from even the deepest groundwater flow paths is available for transpiration in the riparian zone. Recent modifications to RHESSys do allow for groundwater stores to be routed through a defined riparian zone, with improved estimates of concentrations of nitrate and dissolved organic carbon, but the effects on recession signatures have not yet been analysed. It will also be necessary to analyse potential seasonal dynamics in nonlinearity across a wide variety of watersheds to ensure that this signal is not an anomaly and to analyse recession behaviour in relation to robust, representative measures of soil moisture, and the water table to determine the potential physical reality of this model-derived conceptual model.

5 | CONCLUSION

Through analysis of temporal variability in streamflow recession and watershed-scale hydrological and climatological features of a headwater catchment in the southern Appalachian Mountains, which has unique, long-term data on precipitation, streamflow, and soil moisture, we identified systematic seasonal shifts in recession curve characteristics. Our results indicate the following:

1 Rates of ET and antecedent watershed wetness conditions each independently correlate with streamflow recession characteristics.

2 Transpiration is most strongly correlated with streamflow decay in the early growing season when the water table is highest and rates of transpiration are elevated, whereas watershed wetness conditions are most strongly correlated with streamflow decay in the late growing season when the water table is most depressed, not in the nongrowing season as we originally hypothesized.

Using output from the physically based RHESSys model, we described the biophysical processes underlying these shifts and extended previous work on the seasonally transient effects of transpiration of increasing streamflow recession by making the novel observation that such an effect produces hysteresis in streamflow recession curves, governed by both rates of transpiration and watershed wetness conditions, a seemingly fundamental feature of fluvial hydrology, which had gone undocumented. These seasonal hysteretic loops obfuscate the covariance of recession variables when data are analysed in aggregate, an effect that likely explains the failure to find significant relationships between recession characteristics and hydroclimatological features in some previous studies. Future assessments of recession curves according to this temporally variable framework may allow for a more nuanced investigation into the physical drivers of streamflow as well as provide for practical benefits including more accurate model calibration, predictions of water availability, and estimates of stream network extent.

ACKNOWLEDGMENT

"Research presented in this paper was supported by the National Science Foundation Long-Term Ecological Research program (DEB-0823293) granted to the Coweeta LTER Program at the University of Georgia and by the USDA Forest Service, Southern Research Station, Coweeta Hydrologic Laboratory. We acknowledge the support of the USDA Forest Service for providing long-term hydrologic and climate data."

DATA AVAILABILITY STATEMENT

The data that support the findings of this study are available USDA Forest Service Research Data Archive at https://www.fs.usda.gov/rds/archive/Catalog according to the following DOIs: https://doi.org/10.2737/RDS-2017-0031 and https://doi.org/10.2737/RDS-2016-0025, and https://doi.org/10.2737/RDS-2015-0042.

ORCID

Arik Tashie https://orcid.org/0000-0002-7883-3198

REFERENCES

Band, L. E., Patterson, P., Nemani, R., & Running, S. W. (1993). Forest ecosystem processes at the watershed scale: Incorporating hillslope hydrology. Agricultural and Forest Meteorology, 63(1-2), 93-126. https://doi.org/10.1016/0168-1923(93)90024-C

- Bart, R., & Hope, A. (2014). Inter-seasonal variability in baseflow recession rates: The role of aquifer antecedent storage in central California watersheds. *Journal of Hydrology*, 519, 205–213. https://doi.org/10. 1016/i.jhydrol.2014.07.020
- Berry, Z. C., Evaristo, J., Moore, G., Poca, M., Steppe, K., Verrot, L., ... McDonnell, J. (2017). The two water worlds hypothesis: Addressing multiple working hypotheses and proposing a way forward. *Ecohydrology*, 11, e1843. https://doi.org/10.1002/eco.1843
- Biswal, B., & Kumar, D. N. (2014). What mainly controls recession flows in river basins? Advances in Water Resources, 65, 25–33. https://doi.org/ 10.1016/j.advwatres.2014.01.001
- Biswal, B., & Marani, M. (2010). Geomorphological origin of recession curves. Geophysical Research Letters, 37, L24403. https://doi.org/10.1029/2010GL045415
- Bond, B. J., Jones, J. A., Phillips, N., Post, D., & McDonnell, J. J. (2002). The zone of vegetation influence on baseflow revealed by diel patterns of streamflow and vegetation water use in a headwater basin. Hydrological Processes, 16, 1671–1677.
- Boulton, A. J. (2003). Parallels and contrasts in the effects of drought on stream macroinvertebrate assemblages. *Freshwater Biology*, 48, 1173–1185. https://doi.org/10.1046/j.1365-2427.2003.01084.x
- Brooks, J., Barnard, H., Coulombe, R., & McDonnell, J. (2010). Ecohydrologic separation of water between trees and streams in a Mediterranean climate. *Nature Geoscience*, 3, 100–104. https://doi. org/10.1038/ngeo722
- Brutsaert, W., & Nieber, J. L. (1977). Regionalized drought flow hydrographs from a mature glaciated plateau. *Water Resources Research*, 13, 637–644. https://doi.org/10.1029/WR013i003p00637
- Clark, M. P., Rupp, D. E., Woods, R. A., Tromp-van Meerveld, H. J., Peters, N. E., & Freer, J. E. (2009). Consistency between hydrological models and field observations: Linking processes at the hillslope scale to hydrological responses at the watershed scale. *Hydrological Processes*, 23, 311–319. https://doi.org/10.1002/hyp.7154
- Day, F. P., & Monk, C. D. (1974). Vegetation patterns on a southern Appalachian watershed. *Ecology*, *55*, 1064–1074.
- Day, F. P., Phillips, D. L., & Monk, C. D. (1988). Forest communities and patterns. "Forest hydrology and ecology at Coweeta" (pp. 141–149). New York: Springer.
- Dralle, D. N., Karst, N. J., Charalampous, K., Veenstra, A., & Thompson, S. E. (2017). Event-scale power law recession analysis: Quantifying methodological uncertainty. *Hydrology and Earth System Sciences*, 21, 65–81. https://doi.org/10.5194/hess-21-65-2017
- Dralle, D. N., Karst, N. J., & Thompson, S. E. (2015). a, b careful: The challenge of scale invariance for comparative analyses in power law models of the streamflow recession. *Geophysical Research Letters*, 42, 9285–9293. https://doi.org/10.1002/2015GL066007
- Dralle, D. N., Karst, N. J., & Thompson, S. E. (2016). Dry season streamflow persistence in seasonal climates. *Water Resources Research*, *52*, 90–107. https://doi.org/10.1002/2015WR017752
- Eckhardt, K. (2005). How to construct recursive digital filters for baseflow separation. *Hydrological Processes*, *19*, 507–515. https://doi.org/10. 1002/hyp.5675
- Evaristo, J., Jasechko, S., & McDonnell, J. J. (2015). Global separation of plant transpiration from groundwater and streamflow. *Nature*, 525, 91–94. https://doi.org/10.1038/nature14983
- Federer, C. A. (1973). Forest transpiration greatly speeds streamflow recession. *Water Resources Research*, *9*, 1599–1604. https://doi.org/10.1029/WR009i006p01599
- Ford, C. R., Elliott, K. J., Clinton, B. D., Kloeppel, B. D., & Vose, J. M. (2012). Forest dynamics following eastern hemlock mortality in the southern Appalachians. Oikos, 121, 523–536.
- Ford, C. R., Hubbard, R. M., & Vose, J. M. (2011). Quantifying structural and physiological controls on variation in canopy transpiration among planted pine and hardwood species in the southern Appalachians. *Ecohydrology*, 4, 183–195.

- Ghosh, D. K., Wang, D., & Zhu, T. (2016). On the transition of base flow recession from early stage to late stage. *Advances in Water Resources*, 88, 8–13. https://doi.org/10.1016/j.advwatres.2015.11.015
- Godsey, S. E., & Kirchner, J. W. (2014). Dynamic, discontinuous stream networks: hydrologically driven variations in active drainage density, flowing channels and stream order. *Hydrological Processes* 28, 23, 5791–5803.
- Hatcher, R. D. (1988). Bedrock geology and regional geologic setting of Coweeta Hydrologic Laboratory in the eastern Blue Ridge. "Forest hydrology and ecology at Coweeta," (pp. 81–92). New York: Springer.
- Hewlett, J. D., & Hibbert, A. R. (1963). Moisture and energy conditions within a sloping soil mass during drainage. *Journal of Geophysical Research*, 68, 1081–1087. https://doi.org/10.1029/JZ068i004p01081
- Hewlett, J. D., & Hibbert, A. R. (1967). Factors affecting the response of small watersheds to precipitation in humid areas. Forest Hydrology, 1, 275–290.
- Hornbeck, J. W., Adams, M. B., Corbett, E. S., Verry, E. S., & Lynch, J. A. (1993). Long-term impacts of forest treatment on water yield: A summary for northeastern USA. *Journal of Hydrology*, 150, 323–344. https://doi.org/10.1016/0022-1694(93)90115-P
- Hwang, T., Song, C., Vose, J. M., & Band, L. E. (2011). Topographymediated controls on local vegetation phenology estimated from MODIS vegetation index. *Landscape ecology*, 26, 541–556.
- Kirchner, J. W. (2009). Catchments as simple dynamical systems: Catchment characterization, rainfall-runoff modeling, and doing hydrology backward. Water Resources Research, 45, 1–34. https://doi.org/10.1029/2008WR006912
- Konrad, C., & Booth, D. (2005). Hydrological changes in urban streams and their ecological significance. American Fisheries Society Symposium, 47, 157–177.
- Krakauer, N. Y., & Temimi, M. (2011). Stream recession curves and storage variability in small watersheds. *Hydrology and Earth System Sciences*, 15, 2377–2389. https://doi.org/10.5194/hess-15-2377-2011
- McDonnell, J. J. (2014). The two water worlds hypothesis: ecohydrological separation of water between streams and trees? *Water*, 1, 323–329.
- McMillan, H., Gueguen, M., Grimon, E., Woods, R., Clark, M., & Rupp, D. E. (2014). Spatial variability of hydrological processes and model structure diagnostics in a 50 km2 catchment. *Hydrological Processes*, 28, 4896–4913. https://doi.org/10.1002/hyp.9988
- McMillan, H. K., Clark, M. P., Bowden, W. B., Duncan, M., & Woods, R. A. (2010). Hydrological field data from a modeller's perspective: Part 1. Diagnostic tests for model structure. *Hydrological Processes*, 25, 511–522
- Neitsch, S. L., Arnold, J. G., Kiniry, J. R., & Williams, J. R. (2005). Soil and water assessment tool theoretical documentation, Version 2000. Temple, TX: Grassland, soil and water research service.
- Price, K. (2011). Effects of watershed topography, soils, land use, and climate on baseflow hydrology in humid regions: A review. *Progress in Physical Geography*, 35, 465–492. https://doi.org/10.1177/0309133311402714
- Rutledge, A. T., & Mesko, T. O.. (1996). Estimated hydrological characteristics of shallow aquifer systems in the Valley and Ridge, the Blue Ridge, and the Piedmont Physiographic Provinces based on analysis of streamflow recession and base flow, U.S. Geological Survey Professional Paper, 1422 B.
- Sawaske, S. R., & Freyberg, D. L. (2014). An analysis of trends in baseflow recession and low-flows in rain-dominated coastal streams of the pacific coast. *Journal of Hydrology*, 519, 599–610. https://doi.org/10. 1016/j.jhydrol.2014.07.046
- Scaife, S. I., & Band, L. E. (2017). Nonstationarity in threshold response of stormflow in southern Appalachian headwater catchments. Water Resources Research, 53, 6579–6596. https://doi.org/10.1002/ 2017WR020376
- Shaw, S. B. (2016). Investigating the linkage between streamflow recession rates and channel network contraction in a mesoscale catchment in

- New York state. *Hydrological Processes*, 30, 479–492. https://doi.org/10.1002/hyp.10626
- Shaw, S. B., & Riha, S. J. (2012). Examining individual recession events instead of a data cloud: Using a modified interpretation of *dQ/dt-Q* streamflow recession in glaciated watersheds to better inform models of low flow. *Journal of Hydrology*, 434-435(C), 46–54. https://doi.org/10.1016/j.jhydrol.2012.02.034
- Stoelzle, M., Stahl, K., & Weiler, M. (2013). Are streamflow recession characteristics really characteristic? *Hydrology and Earth System Sciences*, 17, 817–828. https://doi.org/10.5194/hess-17-817-2013
- Swank, W. T., & Crossley, D. A. (1988). Introduction and site description. In *Forest hydrology and ecology at Coweeta*, (pp. 3–16). New York: Springer.
- Szilagyi, J., Parlange, M. B., & Albertson, J. D. (1998). Recession flow analysis for aquifer parameter determination. Water Resources Research, 34, 1851–1857. https://doi.org/10.1029/98WR01009
- Tague, C., & Band, L. (2004). RHESSys: Regional hydro-ecologic simulation system—An object-oriented approach to spatially distributed modeling of carbon, water, and nutrient cycling. *Earth Interactions*, 8, 1–42. https://doi.org/10.1175/1087-3562(2004)8<1:RRHSSO>2.0.CO;2
- Tague, C., & Grant, G. (2004). A geological framework for interpreting the low-flow regimes of Cascade streams, Willamette River Basin, Oregon. Water Resources Research, 40, W04303. https://doi.org/10.1029/ 2003WR002629
- Tallaksen, L. M. (1995). A review of baseflow recession analysis. *Journal of Hydrology*, 165, 349–370. https://doi.org/10.1016/0022-1694(94) 02540-R
- Tashie, A. M., Mirus, B. B., & Pavelsky, T. M. (2016). Identifying long-term empirical relationships between storm characteristics and episodic groundwater recharge. Water Resources Research, 52, 21–35. https://doi.org/10.1002/2015WR017876
- Troch, P. A., De Troch, F. P., & Brutsaert, W. (1993). Effective water table depth to describe initial conditions prior to storm rainfall in humid regions. Water Resources Research, 29, 427–434. https://doi.org/10. 1029/92WR02087

- Velbel, M. A. (1988). Weathering and soil-forming processes. In *Forest hydrology and ecology at Coweeta* (pp. 93–102). New York: Springer.
- Vogel, R. M., & Kroll, C. N. (1992). Regional geohydrologic-geomorphic relationships for the estimation of low-flow statistics. Water Resources Research, 28, 2451–2458. http://doi.org/10.1029/92WR01007
- Wang, D. (2011). On the base flow recession at the Panola Mountain Research Watershed, Georgia, United States. Water Resources Research. 47. W03527.
- Wigmosta, M. S., Vail, L. W., & Lettenmaier, D. P. (1994). A distributed hydrology-vegetation model for complex terrain. Water Resources Research, 30, 1665–1679. https://doi.org/10.1029/94WR00436
- Wittenberg, H., & Sivapalan, M. (1999). Watershed groundwater balance estimation using streamflow recession analysis and baseflow separation. *Journal of Hydrology*, 219, 20–33. https://doi.org/10.1016/S0022-1694(99)00040-2
- Wondzell, S. M., Gooseff, M. N., & McGlynn, B. L. (2007). Flow velocity and the hydrologic behavior of streams during baseflow. *Geophysical Research Letters*, 34, L24404. https://doi.org/10.1029/2007GL031256

SUPPORTING INFORMATION

Additional supporting information may be found online in the Supporting Information section at the end of this article.

How to cite this article: Tashie A, Scaife CI, Band LE. Transpiration and subsurface controls of streamflow recession characteristics. *Hydrological Processes*. 2019;33:2561–2575. https://doi.org/10.1002/hyp.13530